TOXICOLOGICAL SCIENCES **125(2)**, 450–461 (2012)
doi:10.1093/toxsci/kfr251
Advance Access publication September 28, 2011

Aerosolized ZnO Nanoparticles Induce Toxicity in Alveolar Type II Epithelial Cells at the Air-Liquid Interface

Yumei Xie,* Nolann G. Williams,* Ana Tolic,* William B. Chrisler,† Justin G. Teeguarden,† Bettye L.S. Maddux,‡ Joel G. Pounds,† Alexander Laskin,* and Galya Orr*,[1]

*Environmental Molecular Sciences Laboratory; †Biological Sciences Division, Pacific Northwest National Laboratory, Richland, Washington 99352; and ‡Materials Science Institute, University of Oregon, Eugene, Oregon 97403

[1]To whom correspondence should be addressed at Environmental Molecular Sciences Laboratory, Pacific Northwest National Laboratory, PO Box 999 MS: K8-88, Richland, WA 99352. Fax: (509) 371-6145, E-mail: galya.orr@pnnl.gov.

Received April 28, 2011; accepted September 18, 2011

The majority of *in vitro* studies characterizing the impact of engineered nanoparticles (NPs) on cells that line the respiratory tract were conducted in cells exposed to NPs in suspension. This approach introduces processes that are unlikely to occur during inhaled NP exposures *in vivo*, such as the shedding of toxic doses of dissolved ions. ZnO NPs are used extensively and pose significant sources for human exposure. Exposures to airborne ZnO NPs can induce adverse effects, but the relevance of the dissolved Zn^{2+} to the observed effects *in vivo* is still unclear. Our goal was to mimic *in vivo* exposures to airborne NPs and decipher the contribution of the intact NP from the contribution of the dissolved ions to airborne ZnO NP toxicity. We established the exposure of alveolar type II epithelial cells to aerosolized NPs at the air-liquid interface (ALI) and compared the impact of aerosolized ZnO NPs and NPs in suspension at the same cellular doses, measured as the number of particles per cell. By evaluating membrane integrity and cell viability 6 and 24 h post-exposure, we found that aerosolized NPs induced toxicity at the ALI at doses that were in the same order of magnitude as doses required to induce toxicity in submersed cultures. In addition, distinct patterns of oxidative stress were observed in the two exposure systems. These observations unravel the ability of airborne ZnO NPs to induce toxicity without the contribution of dissolved Zn^{2+} and suggest distinct mechanisms at the ALI and in submersed cultures.

Key Words: **ZnO nanoparticles; Zn^{2+}; air-liquid interface; aerosol exposures; toxicity; alveolar epithelial cells.**

Investigation of nanoparticulate toxicity to the respiratory tract *in vitro* and *in vivo* is the most commonly used exposure/response system. Airborne engineered nanoparticles (NPs) that enter the respiratory tract are likely to be deposited in the alveolar region (Donaldson *et al*., 2008; Mercer *et al*., 2010; Oberdörster *et al*., 2005), where alveolar epithelial cells present a vulnerable target for particles that escape scavenging by the alveolar macrophages (Oberdörster *et al*., 2005; Takenaka *et al*., 2001). Experimental exposure/response models *in vitro* include cultured lung cells that are (1) grown and exposed to NPs when submersed in diverse cell culture media with variable supplements, including serum proteins and (2) grown at the air-liquid interface (ALI) and exposed to aerosolized NPs or to NPs dispersed in the growth medium. Experimental exposure/response models *in vivo* include (1) orapharyngeal aspiration, (2) intratracheal instillation, and (3) inhalation under diverse forms of aerosol generation. These key differences in cell environment and NP exposure limit the ability to extrapolate results from *in vitro* studies to pulmonary toxicity in animals or humans.

To date, the majority of *in vitro* studies characterizing the impact of inhaled NPs on these and other cells that line the respiratory tract have been carried out in cells exposed to NPs under submersed culture conditions. Use of routine submersed culture systems to screen and compare NP toxicities in lung cells introduces numerous confounding processes under conditions that may be less relevant to inhaled NP exposures, which occur at the air-lung lining fluid-cell interface. First, distinct coronas of proteins and small molecules are formed at the NP surface depending on the environment. In submersed cultures, the corona will be composed of serum proteins (if used as medium supplement or to impair NP agglomeration) and the small molecules and ions of the individual culture medium. In contrast, inhaled NPs will be coated by a corona of proteins and lipid surfactants found in lung lining fluids. These coronas are likely to modulate the interaction of NPs with cell surfaces and, ultimately, the cellular fate of the NP (Casey *et al*., 2008; Dutta *et al*., 2007; Horie *et al*., 2009; Veranth *et al*., 2007). Second, when delivered in culture medium to submersed cells, NP deposition (cellular dose) is a function of gravity and diffusion; processes modulated by NP density and size, concentration, and exposure duration (Hinderliter *et al*., 2010; Teeguarden *et al*., 2007). Moreover, formation of large agglomerates in the growth medium increases gravitational deposition and exposure in submersed cultures and thereby may alter uptake mechanisms

and capacity (Donaldson *et al*., 2001; Porter *et al*., 2008; Sager *et al*., 2007; Wick *et al*., 2007). These processes create uncertainties that impair dose comparisons between *in vivo* and *in vitro* studies in submersed cultures. Third, NP stability, dissolution, and release of potentially toxic ions are dependent, in part, on fluid pH, composition, and duration of exposure to the fluid. Furthermore, cells grown at the ALI are polarized with an apical surface similar to *in vivo,* which is likely to impact cellular NP fate and response. These major differences between the exposures *in vivo* and in submersed cultures can be eliminated or minimized in aerosolized NP exposures at the ALI.

ZnO NPs are used extensively in diverse commercial applications (Ji and Ye, 2008; Wang, 2004). Therefore, they become a significant source for intended and unintended human exposure. Intratracheal instillation and inhalation of ZnO NPs in the rat elicit potent lung inflammatory or cytotoxic responses that are resolved within days to a month (Cho *et al*., 2010; Sayes *et al*., 2007; Warheit *et al*., 2009). These responses resemble "metal fume fever," induced in humans or rodents exposed to ZnO and other metal oxide fumes (Kuschner *et al*., 1995; Wesselkamper *et al*., 2001). *In vitro* studies in bronchial and alveolar epithelial cell lines, exposed to ZnO NPs in solution, reported that the underlying cellular mechanisms involve oxidative stress and inflammatory responses, DNA damage, and cell death (Hsiao and Huang, 2011; Huang *et al*., 2010; Karlsson *et al*., 2008; Wu *et al*., 2010).

Several *in vivo* and *in vitro* studies attempted to decipher the contribution of the intact NP versus dissolved ions in ZnO NP toxicity. Conflicting results have led to increasing confusion on this issue. *In vivo* oropharyngeal aspiration and intratracheal instillation studies, as well as an *in vitro* study, showed that ZnO NPs that were doped with iron, which slows dissolution, among other possible changes to the particle properties were less toxic than undoped particles (George *et al*., 2010; Xia *et al*., 2011). These observations suggest that shedding of dissolved Zn^{2+} might play a role in ZnO NP toxicity. However, a recent intratracheal instillation study in the rat showed that the NPs-induced eosinophilic inflammation that persisted for a month, whereas the supernatant, containing only dissolved Zn^{2+}, elicited a mild and transient inflammatory response (Cho *et al*., 2011). This observation suggests that the more severe responses are likely to originate from the intact ZnO NPs rather than the dissolved ions.

In vitro studies attempting to distinguish between the contribution of the intact NP and the dissolved ions to ZnO NP toxicity reported conflicting results. Studies in alveolar and bronchial epithelial cell lines and in primary alveolar epithelial cells showed cytotoxic and inflammatory responses and severe cellular injury in response to both the NPs and the medium supernatant, as well as Zn^{2+} solutions, suggesting that the toxicity *in vitro* is likely to be mediated, at least in part, by the dissolved Zn^{2+} (Cho *et al*., 2011; Kim *et al*., 2010). However, the exposure of alveolar epithelial cells to $ZnSO_4$ in culture induced cell death at Zn^{2+} concentrations that were much higher than the Zn^{2+} concentrations shed by the NPs at toxic NP concentrations, suggesting that the dissolved Zn^{2+} is unlikely to be a major contributor to the oxidative stress observed in response to the NPs (Lin *et al*., 2009). In support of the view that different mechanisms underlie the cellular responses to the intact or dissolved NPs, a study in alveolar epithelial cells showed differential induction of interleukin (IL)-8 and hemeoxygenase-1 (HO-1) messenger RNA expression in response to ZnO NPs presented to the cells either at the ALI as aerosolized NPs or in submersed conditions as NPs in suspension (Lenz *et al*., 2009).

The confusion that still exists about the origin of airborne ZnO NP toxicity *in vivo* is therefore unlikely to be resolved by *in vitro* studies of NPs that are presented to the cells in solution. To more closely mimic *in vivo* exposures to airborne NPs, we established the exposure of alveolar type II epithelial cells (C10) to aerosolized NPs at the ALI. The mouse C10 alveolar type II epithelial cell line was used because it synthesizes and secretes lung surfactants, and it would enable comparison to future inhalation studies in mice. The objective of our study was to compare the cellular response to ZnO NPs in submersed cultures with the response to aerosolized NPs at the ALI to determine the degree of the intact airborne NP toxicity under conditions that closely mimic inhaled NP exposures *in vivo*. We also compared oxidative stress dynamics in response to NP suspension in submersed cultures and to aerosolized NPs at the ALI to determine whether differences exist in mechanisms underlying toxicity in the two exposure systems.

MATERIALS AND METHODS

Experimental Design

The exposure of alveolar type II epithelial cells (C10) to aerosolized NPs at the ALI was established using commercial modules and in-house design to optimize the efficiency and uniformity of NP delivery while preserving the health of the cells.

Cells grown on membrane inserts were exposed to aerosolized ZnO NPs at the ALI and to ZnO NP solution in submersed cultures. Cellular response was evaluated in the two exposure systems at the same cellular dose, measured as aggregates per unit area using scanning electron microscopy (SEM) to image EM grids that were placed randomly over the cells before exposure. This dose metric enabled accurate comparison of endpoints in the two exposure systems in response to NP dose range that was commonly reported in the literature. Cell proliferation, cell viability, membrane integrity, and oxidative stress were used as endpoints. The MTS assay was used to quantify cell proliferation, propidium iodide (PI)/Hoechst staining was used to quantify cell viability, and the lactate dehydrogenase (LDH) assay was used to determine membrane integrity at 6 and 24 h post-exposure. Measurements were averaged across membrane inserts showing the same number of aggregates per 20 μm^2. These endpoints were used to identify the smallest dose that induced toxicity in each of the exposure systems for comparing toxicity of airborne NPs with toxicity of NPs in solution where global dissolution occurs. The comparison enabled to determine the degree of the intact aerosolized NP toxicity relative to the toxicity of the NPs and their ions in solution. Dichlorofluorescein (DCF) was used to quantify reactive oxygen species (ROS) to determine the degree of oxidative stress over 24 h. This endpoint was measured in the two exposure systems and compared with determine whether distinct mechanisms underlie toxicity at the ALI and in submersed cultures.

Reagents

PI, Hoechst 33258, and RPMI growth medium were purchased from Invitrogen (Carlsbad, CA). CytoTox 96 Non-Radioactive Cytotoxicity Assay CellTiter 96 AQueous Non-Radioactive Cell Proliferation Assay and 5-(and-6)-chloromethyl-2′,7′-dichlorodihydrofluorescein diacetate, acetyl ester (CM-H2DCFDA) were purchased from Promega (Madison, WI). Tert-butyl hydroperoxide (TBHP) was purchased from Acros Organics (New Jersey). Fetal bovine serum (FBS) was purchased from ATCC (Manassas, VA). L-glutamine, penicillin, streptomycin, and poly-L-lysine hydrobromide were purchased from Sigma (St Louis, MO). Millipore (Billerica, MA) water was sterilized using 0.22-μm cellulose nitrate filter (Corning, Corning, NY). Rabbit antibodies against mouse Surfactant Proteins D (AB3434) and A (AB3420) were purchased from Millipore, and goat Alexa Fluor 488 $F(ab)_2$ fragment anti-rabbit IgG (H+L) (52395A) was purchased from Invitrogen.

Cell Culture

C10, a nontumorigenic alveolar type II epithelial cell line derived from mouse lung, was used in this study. One of the main roles of this cell type is to produce the surfactants that prevent the alveolar collapse with expiration. Using immunofluorescence, the expression of surfactant proteins A and D by the C10 cells was confirmed, as demonstrated in Supplementary figure 1, providing a microenvironment that mimics the environment *in vivo*. The cells were grown in RPMI growth medium supplemented with 10% FBS, 2mM L-glutamine, 100 U/ml penicillin, and 100 μg/ml streptomycin. Cells were seeded on cell culture membrane inserts (BD Falcon, transparent polyethylene terephthalate [PET] membranes, 4.2 cm^2 effective growth area, 0.4 μm pore size, $2.0 \pm 0.2 \times 10^6$ pores/cm^2) with 3 ml growth medium on the basal side and 1.3 ml on the apical side. The cells were kept under submersed conditions until full confluence was reached. Cultures at the ALI then were achieved by removing the apical growth medium and incubating at 37°C and 95% relative humidity in a 5% CO_2 incubator for an additional 24 h before exposure to the NPs. For exposures in submersed conditions, fully confluent cells, grown on the same PET membranes as the cells at the ALI, were covered with 1.3 ml growth media and exposed to the NPs in solution.

The ALI Exposure System

The exposure system for aerosolized NPs is illustrated in Figure 1. The system consists of three main components: (1) a vibrating membrane nebulizer (Aeroneb Lab nebulizer system, Aerogen, Galway, Ireland) that generates aerosolized NPs; (2) Vitrocell exposure chambers (Waldkirth, Germany), where the aerosolized NPs are deposited on the cells; and (3) an airflow system that distributes the aerosolized NPs through the system at a highly controlled rate. Synthetic breathing air (Air Liquid USA Inc., Houston, TX) was directed at 1 l/min into a water bubbler for humidification. From there, the air was transported to the nebulizer for generating the aerosol, which was directed into the three exposure chambers at 10 ml/min using a vacuum pump and a flow regulator. Each exposure chamber was designed to expose one membrane insert to the aerosolized NPs via a "trumpet," which is visible in the open chambers in the inset in Figure 1. The exposure chambers were kept at 32°C using circulating water supplied by a water bath, while the whole system was encased in a heated incubation chamber to keep the entering airflow at 32°C. Following 10–20 min exposure sessions, the cells were returned to the incubator until assayed. It was found that cell death increased with increasing exposure time, and airflow rate beyond 10 ml/min accelerated this process. Therefore, the minimal exposure time required to achieve the dose range used in this study, under 10 ml/min flow rate, was chosen.

Preparation of NP Suspensions

NPs were suspended in sterile water (5 mg/ml) and bath-sonicated (Branson 1210 Ultrasonic Cleaner, Danbury, CT) at room temperature (RT) for 10 min, followed by 2×60 s probe sonication (Misonix Sonicator 3000, Farmingdale, NY) at 15 watts on ice, with a 15 s rest between pulses. For the ALI exposures, the NP solution was diluted 1-, 2-, 10-, 50-, and 100-fold, which roughly corresponded to $\geq$ 1000, 700–900, 400–600, and $\leq$ 120 aggregates/20 μm^2, respectively, during 10–20 min exposure sessions. The final solutions included 5% FBS and 0.02% saline. FBS was added to minimize differences in particle properties presented to the cells at the ALI and in submersed cultures. For submersed exposures, NP concentrations (4, 10, 25, 50, 100, 250, 500, and 1000 μg/ml) were achieved by diluting the NP solution in RPMI growth media containing 10% FBS. Final probe-sonication for 2×60 s on ice was done before exposure.

NP Characterization and Dose Measurements

ZnO NPs (25 nm primary particle diameter) were kindly provided by Dr Jeffrey Zink (University of California, Los Angeles) as part of the National Institute of Environmental Health Sciences Nanotechnology Environmental Health and Safety consortium effort. Before NP exposure, electron microscopy (EM) grids (PELCO Carbon Type B support film grids, Ted Pella, Redding, CA) were placed over the cell monolayer and removed right after exposure for further analysis using SEM (FEI Quanta 3-D FEG dual beam, Hillsboro, Oregon) at 10–30 kV. In submersed exposures, poly-L-lysine coated grids were used, and the grids were dipped once in sterile water to remove salt and other growth media ingredients before imaging. SEM was used to determine the relevant size distribution of the particles as seen by the cells and precisely quantify the exposure dose using Genesis Microanalysis software (EDAX, Mahwah, NJ). The dose metric used for ZnO NPs in this study was aggregates per 20 μm^2, the size of a typical cell. The number of aggregates per unit area was measured postexposure for each membrane insert from the SEM images,

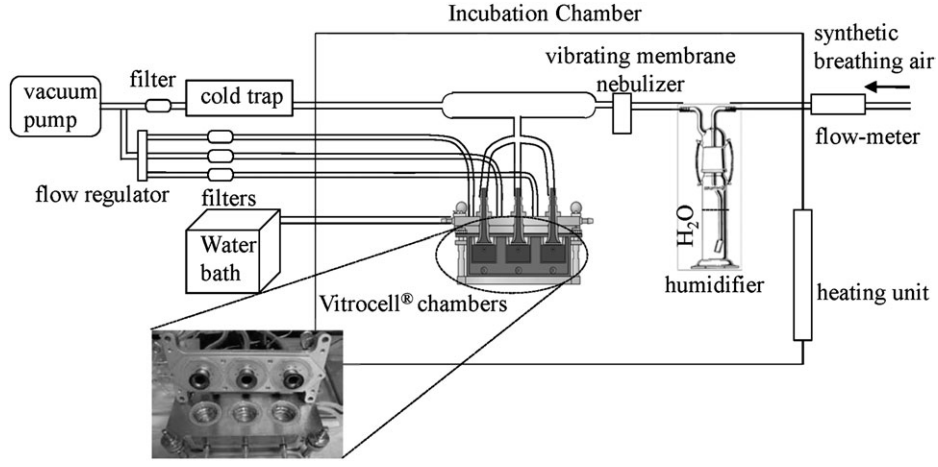

FIG. 1. Illustration of the system for aerosolized nanoparticle exposure at the ALI (refer to ''Materials and Methods'' for details).

taken in both exposure systems. Hydrodynamic size distribution and zeta potential were measured using Zeta PALS (Brookhaven Instruments, Holtsville, NY). Size distribution measurements were done in 5% FBS, 0.2% saline for the ALI, and complete RPMI culture media for submersed conditions.

Toxicity Assessment

Cell proliferation. CellTiter 96 AQueous Non-Radioactive Cell Proliferation Assay was used to determine cell viability 24 h post-exposure through the reduction of MTS (3-(4,5-dimethylthiazol-2-yl)-5-(3-carboxymethoxyphenyl)-2-(4-sulfophenyl)-2H-tetrazolium, inner salt) into aqueous soluble formazan by dehydrogenase enzymes found in metabolically active cells. The MTS solution, in RPMI growth media (1:10 dilution), was added to the apical side of the cells for 1 h incubation at 37°C. Formazan absorbance was measured at 490 nm using a microplate reader (Spectra Max Plus 384, Molecular Devices, Sunnyvale, CA) with multiple reads per well. The mean absorbance of negative control, where cells were exposed to solution or aerosol containing no NPs, was established as 100% cellular viability. The absorbance of cells exposed to the NPs was measured in at least five membrane inserts for each dose, and the values were normalized to negative control. Significant change in the normalized values relative to negative control, determined using the two-tailed Student's *t*-test, indicated a significant change in cell proliferation or viability.

Cell death. A double stain of PI and Hoechst was used to quantify dead cells at 6 and 24 h post-exposure. PI was added to RPMI growth media at 1:1000 dilution, and the solution was placed on the apical side of the cell culture. After 10 min incubation at 37°C, the cells were counterstained with Hoechst to quantify total cell number. The cells were visualized using fluorescence microscopy (Axio Observer, Carl Zeiss, Germany), where the Hoechst emission was collected at 480/40 nm and the PI emission was collected at 629/62 nm. PI- and Hoechst-positive cells were counted in images taken from three membrane inserts for each dose, and the percent of dead cells was quantified as the percent of PI positive cells from the total Hoechst-stained cells. Significant change in cell death, an indicator for toxic response, was determined relative to negative control using the two-tailed Student's *t*-test.

Membrane integrity. CytoTox 96 Non-Radioactive Cytotoxicity Assay was used to quantify LDH release at 6 and 24 h post-exposure through conversion of a tetrazolium salt (INT) into a red formazan product. For positive control, lysis solution (0.9% triton X-100) in RPMI growth media was added to the apical side of control cells for 60 min of incubation at 37°C. Before NP exposure, 50 µl from the apical and basal media were taken as well as 6 and 24 h post-exposure and placed in 96-multiwell plates to which substrate mix was added (50 µl). Following a 30 min incubation at RT under light protection, stop solution was added (50 µl), and the formazan absorbance was measured at 490 nm using a microplate reader with multiple reads per well. Absorption values at 6 and 24 h post-exposure were normalized to the values of the same membrane insert before exposure, and significance was determined relative to the time-matched negative control using the two-tailed Student's *t*-test. Significant change in the normalized values relative to negative control indicated a significant change in membrane damage.

Oxidative Stress

ROS generation at the ALI was measured at 2, 4, 6, 8, 14, and 24 h post-exposures through the oxidation of the cell-permeant compound 5-(and-6)-chloromethyl-2′,7′-dichlorodihydrofluorescein diacetate, acetyl ester (CM-H2DCFDA or DCF). Low (106 aggregate/20 μm^2) and high (933 aggregate/20 μm^2) exposure doses were used. 25µM CM-H2DCFDA was added to the apical growth media and incubated for 30 min at 37°C under light protection. The medium was removed from the apical side, and the cells were trypsinized until fully detached and resuspended in 1 ml RPMI growth media. Positive control was treated with 4.7mM TBHP 60 min before the addition of DCF. All cell samples were centrifuged (IEC Centa MP4R) at 1000 rpm for 2 min and resuspended in 0.5 ml growth media with PI at 1 µg/ml. Positive control for PI was prepared by mixing 1 ml of cell suspension with 5 ml of methanol for 30 min at RT followed by centrifugation and resuspension in 0.5 ml of growth media with 1 µg of PI per ml. DCF and PI fluorescence were measured by flow cytometry using the Influx (BD Biosciences, Seattle, WA). Forward and side scatter were used to gate out cellular debris, and a secondary gate, based on PI emission at 585/29 nm when excited with a 561- nm laser, was generated to differentiate between the live and dead cell populations. DCF fluorescence was measured at 520/15 nm when excited with a 488 nm laser. Gating and median calculations from 30,000 cells were done using Flow Jo software (Tree Star, Ashland, OR). Median fluorescence values, indicating relative degree of ROS, were normalized to time-matched negative control and significance was determined using two-ways ANOVA. A significant change in these values indicated a significant change in oxidative stress.

Statistical Analysis

Data is presented as mean ± SD. The two-tailed Student's *t*-test was used to compare two group means. ANOVA was performed to compare the significance of differences between multiple (≥ 3) groups. For all statistical analyses, p values of less than 0.05 were considered significant.

RESULTS

Size Distribution and Actual Dose of Aerosolized ZnO NPs Were Measured in Particles Settled on EM Grids

EM grids were placed randomly on the cell monolayer before exposures, either at the ALI or in submersed cultures, to enable accurate measurements of particle size distributions and actual cellular doses. The grids were removed at the end of the exposure session and visualized using scanning EM. Figure 2 presents the log-normal size distributions measured from aerosolized particles that landed on the grids at the ALI (Fig. 2A) or in submersed cultures (Fig. 2B). In both cases, NP aggregates were formed. The size distribution at the ALI was measured under high exposure dose of 930 aggregates per 20 μm^2, or per area of an average cell, showing median diameter of 117 nm with geometric standard deviation of 2.17. A similar size distribution was found in submersed conditions (115 nm, $\sigma = 2.43$) under low exposure dose of about 54 aggregates per 20 μm^2. Unlike the median diameter of aerosolized NP aggregates, which did not change with exposure dose, the median diameter of the aggregates in solution inevitably increased at high NP concentrations. Transmission EM images of aerosolized NP aggregates that settled at the ALI are shown in Figure 2C. Dynamic light scattering measurements, which are dominated by the larger particles, showed an average size distribution of 288.2 ± 2.4 nm for the particles in the aerosol solution (5% FBS, 0.2% saline) and 265.7 ± 3.6 nm in the RPMI growth medium containing FBS. Zeta potential of −22.11 ± 0.47 mV was found for the particles in the aerosol solution and −8.78 ± 1.18 mV in the growth medium.

EM was also used to quantify the actual cellular dose as number of landed aggregates per unit area. EM grids were placed randomly over the cells in each of the membrane inserts before exposure and were removed and visualized using scanning EM at the end of the exposure sessions. Figure 3 demonstrates the uniform distribution of the aerosolized NP aggregates at the ALI, which was achieved by the exposure system described earlier (refer to "Materials and Methods"). The scanning EM image was taken from a high dose of 930 aggregates per 20 μm^2. The same approach was taken to quantify the actual cellular dose

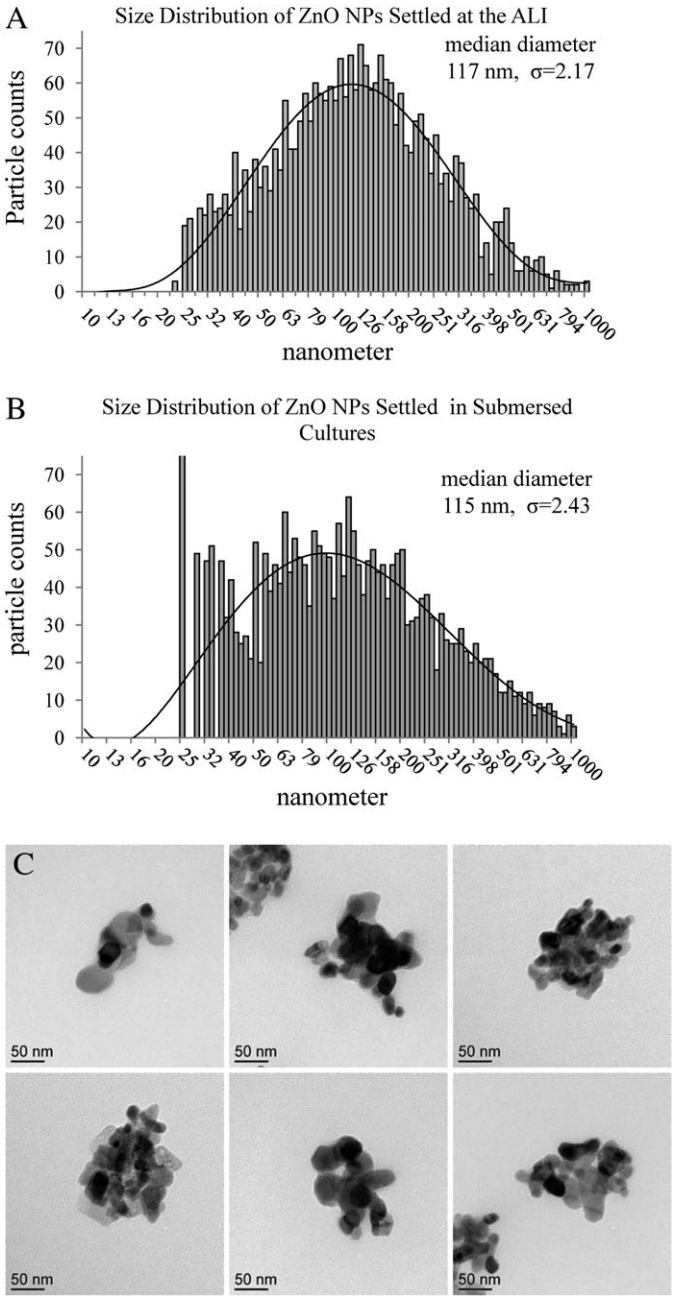

FIG. 2. Size distribution of ZnO NP aggregates as measured from particles that settled on EM grids placed randomly on the cell monolayer either at the ALI (A) or under submersed conditions (B) and imaged using scanning EM. (A) 117 nm ($\sigma = 2.17$) median diameter is found for aerosolized particles measured from high exposure dose of about 900 aggregates per 20 μm^2 or per area of an average cell. (B) A similar median diameter (115 nm, $\sigma = 2.43$) is found for particles in solution when measured from low exposure dose of about 54 aggregates per 20 μm^2. (C) Selected transmission electron micrographs of settled aerosolized ZnO aggregates at the ALI.

in submersed cultures, where the NP doses added to the growth medium were measured in μg/ml. EM grids, coated with poly-L-lysine to ensure NP adherence, were placed on the cell before

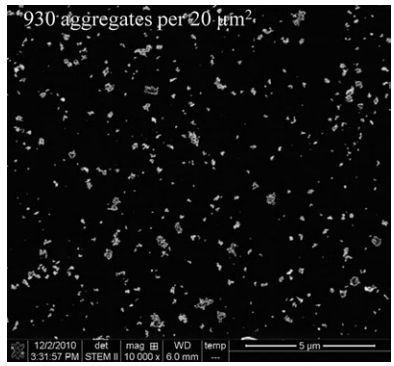

FIG. 3. Scanning electron micrograph demonstrating the uniform distribution achieved using the system for aerosolized NP exposure at the ALI. The image was taken from a high exposure dose, where 930 aggregates per 20 μm^2 were formed. Such images were used to determine exposure dose for each membrane insert as the number of settled aggregates per cell.

adding the NPs to the growth medium. The number of aggregates per 20 μm^2 found for each of the doses used in submersed cultures is listed in Table 1.

Responses to Aerosolized NPs at the ALI Were Compared with Responses in Submersed Cultures at the Same Number of Settled NP Aggregates per Cell

Toxicity of aerosolized ZnO NPs was assessed in alveolar type II epithelial cells grown at the ALI. These cells, which produce surfactants that prevent the alveolar collapse with expiration (Weaver and Whitsett, 1991; Wikenheiser *et al.*, 1993), present a target cell type for inhaled NPs *in vivo*. Membrane integrity was measured by the release of LDH into the basal medium at 6 and 24 h post-exposure. As shown in Figure 4A, a significant deterioration in membrane integrity was detected 24 h post-exposure when the dose reached about 500 aggregates per 20 μm^2 ($p = 0.0020$). A higher dose of 800 aggregates per 20 μm^2 was required to detect significant membrane damage at 6 h post-exposure ($p = 0.0207$). Exposure to aerosolized supernatant, taken from a toxic particle dose of about 800 aggregates per 20 μm^2 and carrying Zn^{2+}, failed to impose membrane damage, indicating that little or no aerosolized supernatant reached the cells, and the membrane's integrity was damaged by exposures to the intact NPs. The conversion of the doses from aggregates/20 μm^2 to mass (μg/cm^2) and surface area (μg/cm^2) is provided in Supplementary table 1.

Cell viability was evaluated in response to aerosolized NPs at the ALI 24 h post-exposure by quantifying the degree of cell proliferation using the MTS assay. As shown in Figure 4B, a significant decrease in cell proliferation was observed when the dose reached about 800 aggregates per 20 μm^2 ($p = 0.0499$). Exposure to aerosolized supernatant obtained from a toxic particle dose of about 800 aggregates per 20 μm^2 elicited no toxic response. As mentioned, this observation indicates that little or no aerosolized supernatant reached the cells, and the toxicity originated from the exposure to the intact NP.

TABLE 1
The Number of Aggregates per 20 μm2 as Quantified by EM for Each of the Doses Used in Submersed Cultures After 1 h From the Addition of the NPs to the Growth Medium

Exposure dose μg/ml	[a]Aggregates/20 μm^2 ± SD
4	0
10	0
25	8 ± 4
50	54 ± 15
100	167 ± 25
250	326 ± 51
500	1165 ± 145

[a]Averaged values from three experiments for each exposure dose.

Exposures to NPs in solution were done in cells grown on the same transwell membrane inserts as the cells at the ALI but instead were submersed under growth media. The particle solution was added to the apical medium and replaced with fresh medium after 1 h to achieve a defined dose of settled aggregates in a short time period. This approach enables the comparison of exposures in submersed cultures with aerosolized NP exposures at the ALI, where a defined number of settled aggregates was achieved within 10–20 min. Ideally, the particle solution in submersed exposures would be removed after 10–20 min as well. However, to achieve high numbers of settled particles in solution in such a short time, it would be necessary to use a very high NP concentration, which leads to larger agglomerates.

As shown in Figure 5A, a significant increase in LDH release into the basal medium was detected 24 h post-exposure when the exposure dose reaches about 300 aggregates per 20 μm^2 ($p = 0.0353$). This number of aggregates per 20 μm^2, which was quantified using EM and is listed in parenthesis, was achieved by adding 250 μg/ml NPs to the apical growth medium and replacing the medium 1 h later. When LDH release was quantified in the apical medium (Fig. 5B), a significant increase was detected 24 h post-exposure in response to an even lower dose of 167 aggregates per 20 μm^2 ($p = 0.0223$). This cellular dose corresponds to 100 μg/ml NPs added to the apical growth medium and replaced with fresh medium 1 h later.

Cell viability was assessed 24 h post-exposure to NPs in solution using the MTS assay. As shown in Figure 5C, a significant decrease in cell proliferation was detected when the cellular dose reached about 300 aggregates per 20 μm^2 ($p = 0.0205$), or 250 μg/ml/1 h, as measured 24 h post-exposure.

Cell viability was also assessed using PI to detect dead cells. Hoechst was used to stain both live and dead cells and enable the calculation of percent PI positive cells from the total cell population. In aerosolized NP exposures at the ALI, a significant decrease in live cells was observed after 24 h in response to doses within the range of 595–1390 aggregates per 20 μm^2 ($p < 0.0001$), as shown in Figure 6A. This observation is in agreement with the MTS assay (Fig. 4B), where a significant decrease in cell viability was observed at about 800 aggregates per 20 μm^2. Exposures in submersed cultures led to a significant decrease in live cells at about 300 aggregates per 20 μm^2 ($p < 0.0001$) (Fig. 6B). This is in agreement with the MTS assay (Fig. 5C), where a significant decrease in cell viability was detected at about 300 aggregates per 20 μm^2. Examples of fluorescence images used to quantify the percent of dead cells (pink) from the total cells (blue) using PI and Hoechst, respectively, are shown in Figure 6C.

The data presented indicates that the numbers of aggregates per 20 μm^2, or per cell, required to achieve a significant deterioration in membrane integrity and cell viability in response to aerosolized NP exposures at the ALI and in submersed conditions were in the same order of magnitude.

Oxidative Stress Was Quantified in Response to Aerosolized ZnO NPs at the ALI and to NP Suspension in Submersed Cultures Over Time

Using DCF, ROS generation was detected and quantified over time in response to aerosolized NP exposures at the ALI and to NP suspension in submersed cultures using flow cytometry. Due to its indiscriminate response to free radicals, DCF is useful in quantifying overall oxidative stress (Wang and Joseph, 1999). The cells were exposed at the ALI to a high dose of 933 aggregates per 20 μm^2 and a low dose of 106 aggregates per 20 μm^2, as determined using EM. In submersed cultures, the cells were exposed to a high dose of 500 μg/ml, which is equivalent to about 1000 aggregates per 20 μm^2, and a low dose of 50 μg/ml, which is equivalent to about 50 aggregates per 20 μm^2. As shown in Figure 7A, a significant increase in oxidative stress was detected in response to the high dose at the ALI 6 h post-exposure ($p < 0.0001$), which decayed back to baseline 8–10 h post-exposure. No significant increase in oxidative stress was detected at the ALI in response to the low dose. LDH measurements in these samples (Fig. 7B) showed a significant decrease in membrane integrity in response to the high dose, but not the low dose, as early as 6 h post-exposure ($p = 0.0259$), which was correlated with the peak in oxidative stress. These observations indicate that the mechanism underlying aerosolized ZnO NP toxicity at the ALI involves a transient increase in oxidative stress that subsides as cell damage takes place.

In contrast to the oxidative stress pattern at the ALI, a robust increase in oxidative stress of more than 10-fold was observed in submersed cultures as early as 2 h post-exposure ($p < 0.01$) (Fig. 7C), which decayed back to baseline 8–10 h post-exposure. Despite the difference in the patterns of oxidative stress at the ALI and in submersed conditions, the pattern of LDH release was similar in both conditions (Fig. 7D), showing a significant increase in LDH release in response to the high dose ($p = 0.0348$)—but not the low dose—as early as 6 h post-exposure.

DISCUSSION

The main new finding to emerge from this work is the ability of aerosolized ZnO NPs to induce toxicity at the ALI at doses that are in the same order of magnitude as those required to

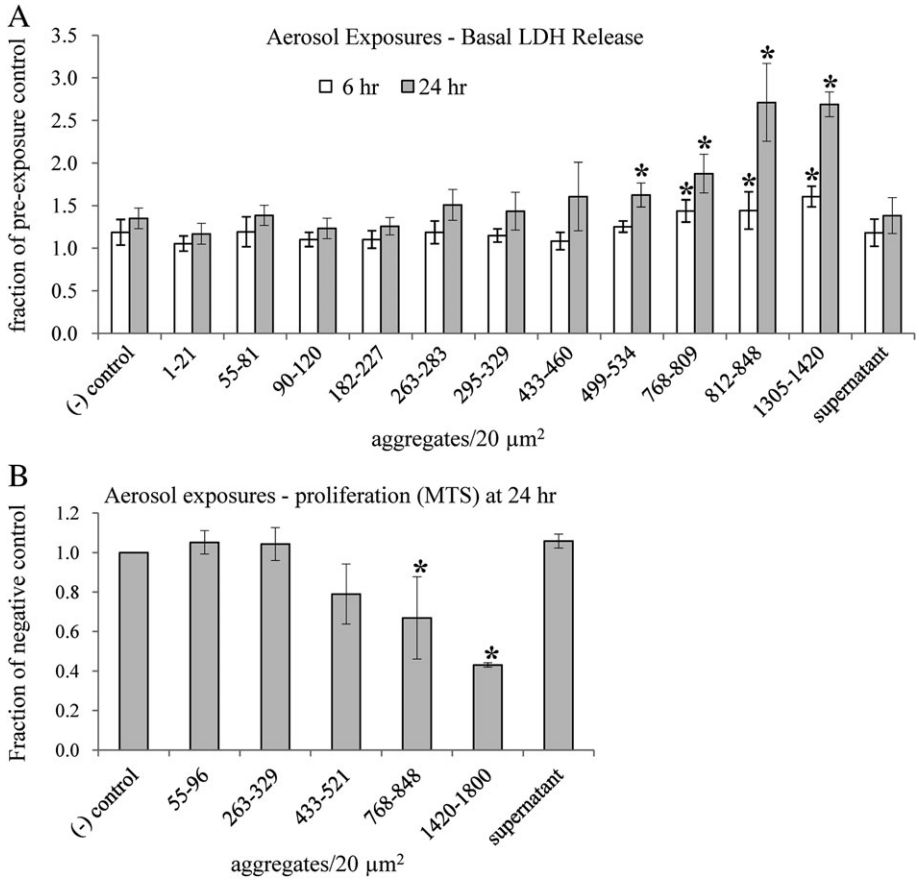

FIG. 4. (A) Aerosolized ZnO NP exposures of alveolar type II epithelial cells at the ALI significantly compromised the integrity of the cell membrane when the exposure dose reached about 500 aggregates per 20 μm^2, as quantified 24 h post-exposure by LDH released into the basal medium ($p = 0.0020$). At 6 h post-exposure, significant compromise in membrane integrity was detected starting at about 800 aggregates per 20 μm^2 ($p = 0.0207$). Exposure to aerosolized supernatant, taken from a toxic particle dose, failed to impose membrane damage, indicating that little or no aerosolized supernatant reached the cells and membrane integrity was compromised by exposures to the intact NPs. LDH measurements for each dose range at each time point were taken from at least three different membrane inserts. The absorbance values were normalized to preexposure measurements, taken for each of the membrane inserts, to correct for normal deterioration that occurs over time. (B) Aerosolized ZnO NP exposures imposed a significant decrease in cell proliferation at the ALI when the exposure dose reached about 800 aggregates per 20 μm^2, as measured by the MTS assay at 24 h post-exposure ($p = 0.0499$). Exposure to aerosolized supernatant obtained from a toxic particle dose showed no decrease in cell proliferation. MTS measurements from at least five different membrane inserts were used for each exposure dose range. These values were normalized to the negative (−) control, where cells were exposed to aerosol containing no particles. Significance was determined for both LDH and MTS measurements using the two-tailed Student's *t*-test with 95% confidence when compared with negative (−) control at the same time point.

induce toxicity in submersed cultures, where both the NPs and the dissolved ions contribute to the observed toxicity. The significance of this finding is that the toxicity of aerosolized ZnO NPs must originate from direct interactions of cellular structures with the intact NP or with locally dissolved Zn^{2+} at the contact site of the NP with the cell rather than from global dissolution. The work clears the confusion created by *in vitro* exposures in submersed cultures by showing that ZnO NP toxicity is not dependent on the massive dissolution of the particles and the production of toxic doses of Zn^{2+}, unraveling the potency of exposures to the intact NPs. Our observations indicate that inhaled ZnO NPs have the potential to induce toxicity by local interactions at the contact site of the NP with cellular structures.

The ALI system that we have established prevented the exposure of the cells to toxic doses of dissolved ions and the formation of large agglomerates, enabling the assessment of airborne NP toxicity at actual cellular dose under conditions that closely mimic the exposure to inhaled NPs *in vivo*. Our approach can also avoid the formation of protein coronas that are formed around NPs in growth media, which mask the original surface properties of the NPs and introduce variability across systems. However, the goal of our study was to compare the impact of aerosolized NPs and NPs in growth medium. Thus, FBS was added to the aerosol solution. By quantifying the number of settled particles per cell, we were able to provide accurate relationships between the actual cellular dose and cellular response. This approach also enabled the comparison of cellular responses at the ALI and in submersed cultures using the same dose metric, measured as the number of settled aggregates per cell. However, an inevitable inaccuracy in the

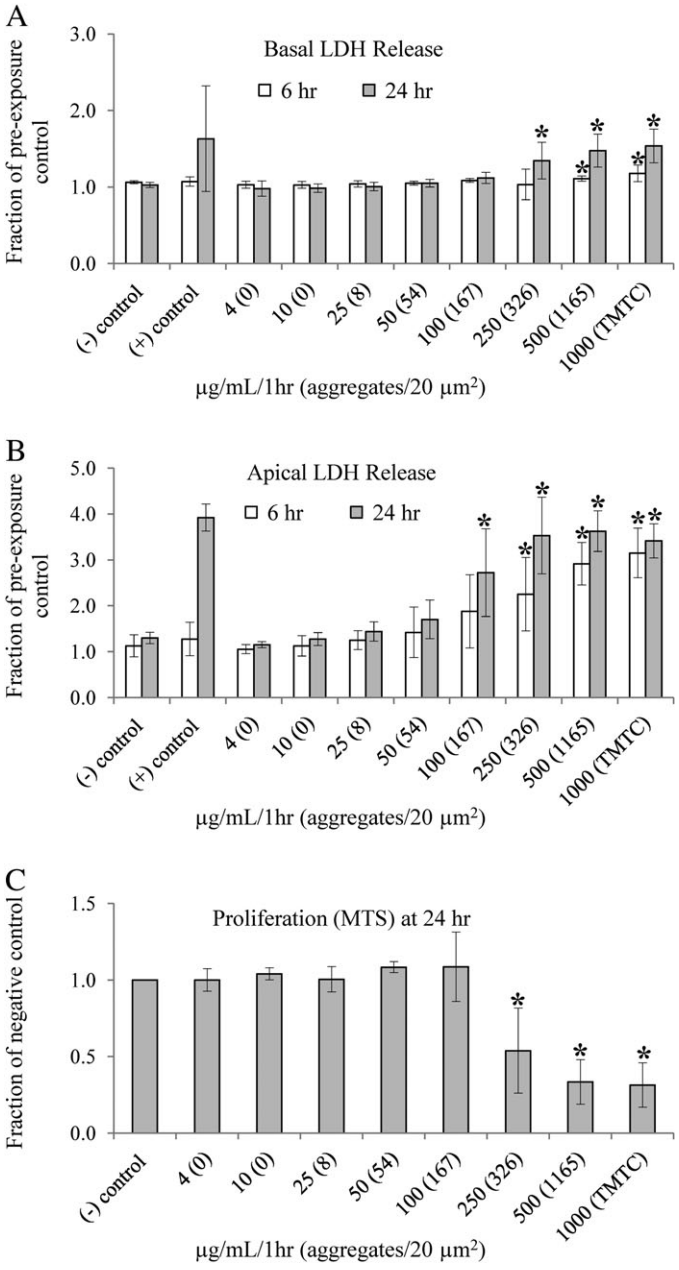

FIG. 5. (A) ZnO NP exposures in solution were done in cells grown on the same transwell membrane inserts as the cells at the ALI but submersed under growth media. A significant increase in LDH release into the basal medium was detected 24 h post-exposure when the exposure dose reached about 300 aggregates per 20 μm^2 ($p = 0.0353$), as quantified by EM and listed in parentheses. This dose was achieved by adding 250 μg/ml NPs to the apical growth medium and replacing the medium 1 h later. (B) When LDH release was quantified in the apical medium, a significant increase was detected 24 h post-exposure at 167 aggregates per 20 μm^2 ($p = 0.0223$). This dose corresponds to 100 μg/ml NPs added to the apical growth medium and replaced with fresh medium 1 h later. At least three different membrane inserts were used for each exposure dose at each time point for both basal and apical LDH measurements. The absorbance values were normalized to preexposure values for each membrane insert to correct for normal cell deterioration. (C) A significant decrease in cell proliferation was detected using the MTS assay when the exposure dose reached about 300 aggregates per 20 μm^2 ($p = 0.0205$), or 250 μg/ml/1 h, as measured 24 h post-exposure. At least five membrane inserts were used for each exposure dose, and the absorbance values were normalized to the negative (−) control, where cells were exposed to solution containing no particles. For both LDH and MTS measurements, significance was determined using the two-tailed Student's *t*-test with 95% confidence when compared with negative (−) control.

conversion of μg/ml to aggregates/20 μm^2 might have been introduced by coating the grids placed in submersed cultures with poly-L-lysine to avoid the loss of the NPs back to the growth medium. The positively charged poly-L-lysine could attract more NPs, leading to larger number of aggregates per unit area than the number of aggregates that were settled on the cells. In addition, an increase in the size of the aggregates occurred in submersed cultures at high NP concentrations. Such increase in aggregate size was not observed in aerosolized NP exposures at the ALI. Therefore, while similar numbers of settled aggregates per cell were compared, larger numbers of NPs were present in submersed conditions at high exposure doses. However, this difference in aggregate size only strengthens our conclusion that the intact aerosolized NP at the ALI is as potent in inducing toxicity, if not more, as the NPs and their massively dissolved ions in solution. Other methods could be used for accurate measurements of the cellular dose at the ALI, such as a quartz crystal microbalance, which would report dose in μg/cm^2. This approach, however, could not be used in submersed culture for supporting an accurate comparison of toxicity in the ALI and submersed cultures. Other methods, such as inductively coupled plasma mass spectrometry, could be used to quantify actual cellular dose in both systems as well. Using aggregates per unit area as the dose metric, measured by EM, enabled the characterization of the aggregate size distribution at the cell surface in both exposure systems.

Our study was conducted over 24 h exposures, showing toxic responses over short time periods. However, *in vivo* studies have shown adverse effects in response to ZnO NPs that were resolved within days to a month (Cho *et al.*, 2010; Sayes *et al.*, 2007; Warheit *et al.*, 2009), indicating the need to assess toxicity over longer time periods. Whether the ALI could provide an appropriate system for assessing transient toxic responses over longer time periods is yet to be determined.

The Tox21 paradigm proposes to utilize high throughput *in vitro* assays and limited *in vivo* studies, mainly focused on pharmacokinetics to rank chemicals and nanomaterial hazards for further evaluation in more complete model systems such as whole animals. The ALI system is expected to serve as an intermediate step between high throughput *in vitro* assay systems, which have been shown to have a number of dosimetry and biology related limitations (Teeguarden *et al.*, 2007) and whole animal systems.

Our work, which identified a clear role for the intact NP in ZnO NP toxicity, also raises the possibility that different mechanisms underlie the toxicity induced by the intact NP and the globally dissolved Zn^{2+}. While studies in submersed conditions show that

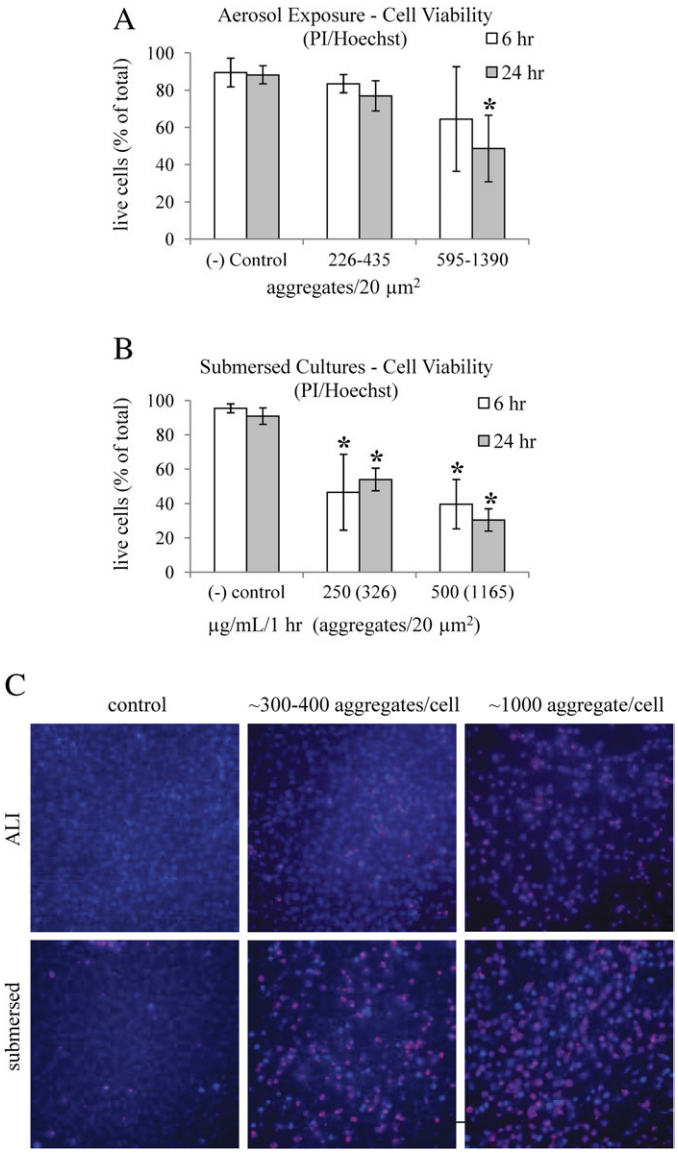

FIG. 6. (A) A significant decrease in live cells was observed at the ALI 24 h after aerosolized NP exposure in response to doses within the range of 595–1390 aggregates per 20 μm^2 ($p < 0.0001$). (B) Exposures in submersed conditions led to a significant decrease in live cells at about 300 aggregates per 20 μm^2 ($p < 0.0001$) as early as 6 h post-exposure. (C) Examples of fluorescence images used to quantify the percent of dead cells (pink) stained with PI from the total cells (blue) stained with Hoechst.

exposures to the NP supernatant or to Zn^{2+} solutions lead to inflammatory responses, cellular injury, and toxicity, just as the exposures to the NPs in solution (Cho *et al.*, 2011; Kim *et al.*, 2010), these outcomes might originate from molecular processes that are distinct from the local processes that occur in response to the intact NP. The dissolved Zn^{2+} in submersed exposures are likely to interact with molecules at multiple sites along the cell membrane and enter the cell through multiple and nonspecific mechanisms. However, the intact NP is likely to interact with specific molecules that are spatially limited to the contact site and enter the cell through endocytic pathways specific to the NPs. This view is supported by the distinct patterns of oxidative stress that we observed at the ALI and in submersed cultures. The robust increase, more than 10-fold, observed in oxidative stress as early as 2 h post-exposure in submersed cultures could be explained by the global and readily available Zn^{2+} in the exposure solution. By contrast, the relatively small and transient increase in oxidative stress at the ALI could be explained by the local and confined processes at the particle contact site with the cell. If NP dissolution occurs at the contact site, the interactions with Zn^{2+} must also be limited to specific molecules and organelles around that site. We have shown previously that specific cell surface molecules mediate the interactions of NPs at the cell surface and their internalization pathways according to the particle surface properties (Orr *et al.*, 2007, 2009, 2011). It is likely that the intact ZnO NP is captured by specific molecules at the cell surface, which dictate the interactions, internalization pathways and intracellular fate of the NP, and ultimately, the response of the cell. In the case of the dissolved ions in submersed conditions, multiple and nonspecific molecules are likely to mediate these processes. In support of the possibility that different mechanisms underlie the toxicity of the intact NP and the globally dissolved ions are observations made in alveolar epithelial cells showing distinct changes in HO-1 and IL-8 gene expression levels when the cells were exposed to aerosolized ZnO NPs at the ALI or to NPs in solution (Lenz *et al.*, 2009). Similarly, observations made in alveolar epithelial cells exposed to $ZnSO_4$ in culture showed toxicity at Zn^{2+} concentrations that were much higher than the Zn^{2+} concentrations shed in the presence of toxic concentrations of the NPs (Lin *et al.*, 2009), unraveling toxicity that originated solely from the intact NPs. The instillation study in the rat where severe and long-lasting inflammatory response was induced by the NPs, but only mild and transient response was induced by the supernatant (Cho *et al.*, 2011), also supports this possibility. These observations unravel a distinct and critical role for the intact NP in ZnO NP toxicity *in vivo*. It is possible, however, that locally dissolved Zn^{2+} around the intact NP contribute to ZnO NP toxicity *in vivo*. This possibility is supported by the aspiration and instillation study, showing reduced toxicity by ZnO NPs that were doped with iron, which slows the dissolution rate of the particles (Xia *et al.*, 2011). However, this study does not exclude the possibility that iron doping might also decrease the interactive sites available to the cell at the NP surface.

While studies in marine and freshwater organisms, which are naturally exposed to NPs in solution, suggest that ZnO NP toxicity could be attributed mainly to the dissolved Zn^{2+} (Aruoja *et al.*, 2009; Franklin *et al.*, 2007; Miao *et al.*, 2010; Wong *et al.*, 2010), other studies in aquatic and soil organisms (Manzo *et al.*, 2010; Poynton *et al.*, 2011; Zhu *et al.*, 2009), as well as in bacteria (Jiang *et al.*, 2009), showed a significant role for both NP and dissolved Zn^{2+}, each with distinct underlying mechanisms (Jiang *et al.*, 2009; Manzo *et al.*, 2010; Poynton *et al.*, 2011). Differentially regulated genes were observed in

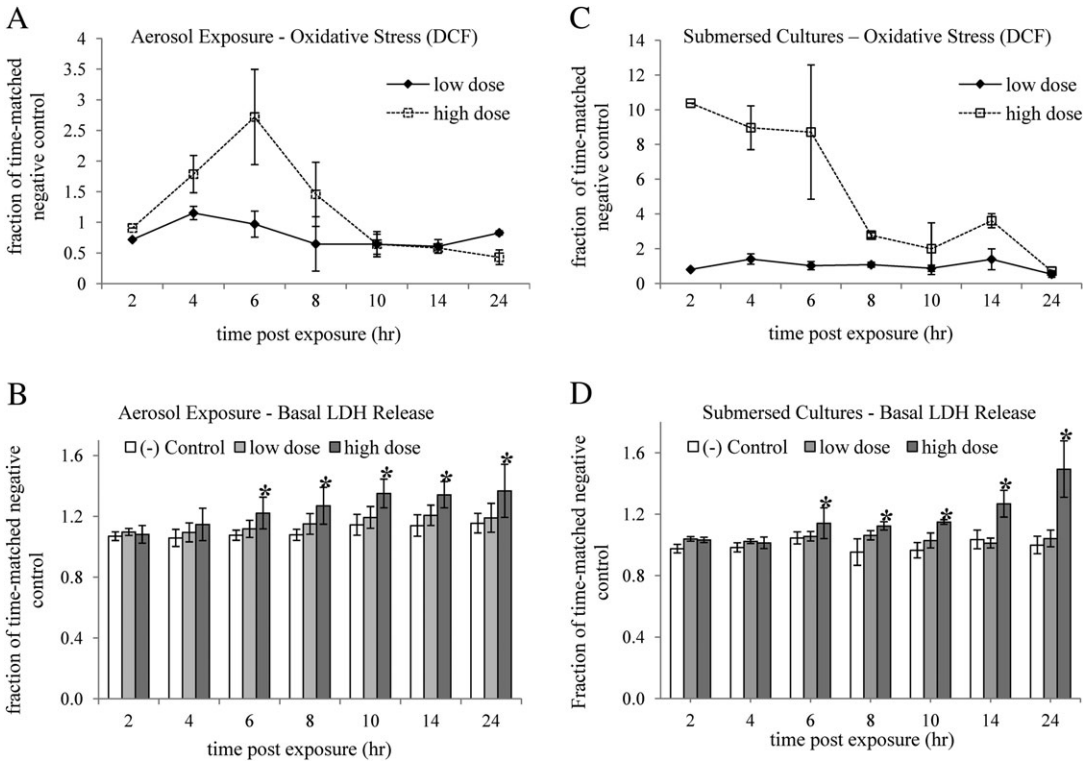

FIG. 7. (A) A significant increase in oxidative stress was detected using DCF in response to high dose (933 aggregates per 20 μm^2) of aerosolized ZnO NPs as early as 6 h post-exposure ($p < 0.0001$). No significant increase in oxidative stress was detected in response to the low dose (106 aggregates per 20 μm^2). Median values from 30,000 cells per time point were normalized to negative control for each time point, and significance was determined using two-ways ANOVA with 95% confidence when comparing to negative control. (B) LDH measurements in these samples showed a significant decrease in membrane integrity in response to the high dose, but not low dose, as early as 6 h post-exposure ($p = 0.0259$), which was correlated with the peak in oxidative stress. LDH measurements were normalized to the negative (−) control, where cells were exposed to aerosol containing no particles. Significance was determined using the two-tailed Student's *t*-test with 95% confidence when compared with the negative (−) control. (C) A robust increase in oxidative stress was detected in submersed cultures in response to the high dose (500 μg/ml or about 1000 aggregates per 20 μm^2) as early as 2 h post-exposure ($p < 0.01$). No increase in oxidative stress was detected in response to the low dose (50 μg/ml or about 50 aggregates per 20 μm^2). (D) As in the aerosolized NP exposures, a significant increase in LDH release was detected in response to the high dose as early as 6 h post-exposure ($p = 0.0348$). No increase in LDH release was detected in response to the low dose.

Daphnia magna, where the genes for multicystatin, ferritin, and C1q-containing gene were regulated in response to the NPs but not the ions (Poynton *et al.*, 2011). Physical perturbations of cellular structures were suggested to underlie the impact of the intact NP versus Zn^{2+} in bacteria and certain soil organisms (Jiang *et al.*, 2009; Manzo *et al.*, 2010). Rapid clearance kinetics of soluble ions was suggested to account for the milder responses observed in rats exposed to the ions versus the NPs by instillation (Cho *et al.*, 2011) and could also explain, in part, differences observed in other organisms. Our study clearly shows that the intact NP plays a critical role in airborne ZnO NP toxicity and demonstrates distinct oxidative stress dynamics at the ALI and in submersed cultures. The distinct spatial and temporal patterns of internalization, molecular interactions, and intracellular fate that are expected for the NPs and the dissolved ions are likely to impact distinct cellular functions. These molecular processes, and whether and how local dissolution occurs and contributes to toxicity, are currently being investigated.

SUPPLEMENTARY DATA

Supplementary data are available online at http://toxsci.oxfordjournals.org/.

FUNDING

National Institute of Environmental Health Sciences (1RC2ES018786-01 to G.O.); Air Force Research Laboratory/Oregon Nanoscience and Microtechnologies Institute/Safer Nanomaterials & Nanomanufacturing Initiative (FA8650-05-1-5041 to B.L.S.M and G.O).

ACKNOWLEDGMENTS

We thank Dr Zink at the University of California, Los Angeles, for providing the ZnO NPs as part of the National Institute of Environmental Health Science Nanotechnology Environmental Health and Safety consortium effort. The research was performed

using the Environmental Molecular Sciences Laboratory, a national scientific user facility sponsored by the Department of Energy's Office of Biological and Environmental Research and located at Pacific Northwest National Laboratory.

REFERENCES

Aruoja, V., Dubourguier, H. C., Kasemets, K., and Kahru, A. (2009). Toxicity of nanoparticles of CuO, ZnO and TiO2 to microalgae Pseudokirchneriella subcapitata. *Sci. Total Environ.* **407,** 1461–1468.

Casey, A., Herzog, E., Lyng, F. M., Byrne, H. J., Chambers, G., and Davoren, M. (2008). Single walled carbon nanotubes induce indirect cytotoxicity by medium depletion in A549 lung cells. *Toxicol. Lett.* **179,** 78–84.

Cho, W. S., Duffin, R., Poland, C. A., Duschl, A., Oostingh, G. J., Macnee, W., Bradley, M., Megson, I. L., and Donaldson, K. (2011). Differential pro-inflammatory effects of metal oxide nanoparticles and their soluble ions in vitro and in vivo; zinc and copper nanoparticles, but not their ions, recruit eosinophils to the lungs. *Nanotoxicology*. doi:10.3109/17435390.2011.552810.

Cho, W. S., Duffin, R., Poland, C. A., Howie, S. E., MacNee, W., Bradley, M., Megson, I. L., and Donaldson, K. (2010). Metal oxide nanoparticles induce unique inflammatory footprints in the lung: Important implications for nanoparticle testing. *Environ. Health Perspect.* **118,** 1699–1706.

Donaldson, K., Borm, P. J. A., Oberdörster, G., Pinkerton, K. E., Stone, V., and Tran, C. L. (2008). Concordance between in vitro and in vivo dosimetry in the proinflammatory effects of low-toxicity, low-solubility particles: The key role of the proximal alveolar region. *Inhal. Toxicol.* **20,** 53–62.

Donaldson, K., Stone, V., Clouter, A., Renwick, L., and MacNee, W. (2001). Ultrafine particles. *Occup. Environ. Med.* **58,** 211–216.

Dutta, D., Sundaram, S. K., Teeguarden, J. G., Riley, B. J., Fifield, L. S., Jacobs, J. M., Addleman, S. R., Kaysen, G. A., Moudgil, B. M., and Weber, T. J. (2007). Adsorbed proteins influence the biological activity and molecular targeting of nanomaterials. *Toxicol. Sci.* **100,** 303–315.

Franklin, N. M., Rogers, N. J., Apte, S. C., Batley, G. E., Gadd, G. E., and Casey, P. S. (2007). Comparative toxicity of nanoparticulate ZnO, bulk ZnO, and ZnCl2 to a freshwater microalga (Pseudokirchneriella subcapitata): The importance of particle solubility. *Environ. Sci. Technol.* **41,** 8484–8490.

George, S., Pokhrel, S., Xia, T., Gilbert, B., Ji, Z. X., Schowalter, M., Rosenauer, A., Damoiseaux, R., Bradley, K. A., Mädler, L., *et al.* (2010). Use of a rapid cytotoxicity screening approach to engineer a safer zinc oxide nanoparticle through iron doping. *ACS Nano* **4,** 15–29.

Hinderliter, P. M., Minard, K. R., Orr, G., Chrisler, W. B., Thrall, B. D., Pounds, J. G., and Teeguarden, J. G. (2010). ISDD: A computational model of particle sedimentation, diffusion and target cell dosimetry for in vitro toxicity studies. *Part. Fibre Toxicol.* **7,** 36.

Horie, M., Nishio, K., Fujita, K., Endoh, S., Miyauchi, A., Saito, Y., Iwahashi, H., Yamamoto, K., Murayama, H., Nakano, H., *et al.* (2009). Protein adsorption of ultrafine metal oxide and its influence on cytotoxicity toward cultured cells. *Chem. Res. Toxicol.* **22,** 543–553.

Hsiao, I. L., and Huang, Y. J. (2011). Effects of various physicochemical characteristics on the toxicities of ZnO and TiO(2) nanoparticles toward human lung epithelial cells. *Sci. Total Environ.* **409,** 1219–1228.

Huang, C. C., Aronstam, R. S., Chen, D. R., and Huang, Y. W. (2010). Oxidative stress, calcium homeostasis, and altered gene expression in human lung epithelial cells exposed to ZnO nanoparticles. *Toxicol. In Vitro* **24,** 45–55.

Ji, S. L., and Ye, C. H. (2008). Synthesis, growth mechanism, and applications of zinc oxide nanomaterials. *J. Mater. Sci. Technol.* **24,** 457–472.

Jiang, W., Mashayekhi, H., and Xing, B. S. (2009). Bacterial toxicity comparison between nano- and micro-scaled oxide particles. *Environ. Pollut.* **157,** 1619–1625.

Karlsson, H. L., Cronholm, P., Gustafsson, J., and Moller, L. (2008). Copper oxide nanoparticles are highly toxic: A comparison between metal oxide nanoparticles and carbon nanotubes. *Chem. Res. Toxicol.* **21,** 1726–1732.

Kim, Y. H., Fazlollahi, F., Kennedy, I. M., Yacobi, N. R., Hamm-Alvarez, S. F., Borok, Z., Kim, K. J., and Crandall, E. D. (2010). Alveolar epithelial cell injury due to zinc oxide nanoparticle exposure. *Am. J. Respir. Crit. Care Med.* **182,** 1398–1409.

Kuschner, W. G., D'Alessandro, A., Wintermeyer, S. F., Wong, H., Boushey, H. A., and Blanc, P. D. (1995). Pulmonary responses to purified zinc oxide fume. *J. Investig. Med.* **43,** 371–378.

Lenz, A. G., Karg, E., Lentner, B., Dittrich, V., Brandenberger, C., Rothen-Rutishauser, B., Schulz, H., Ferron, G. A., and Schmid, O. (2009). A dose-controlled system for air-liquid interface cell exposure and application to zinc oxide nanoparticles. *Part. Fibre Toxicol.* **6,** 32.

Lin, W. S., Xu, Y., Huang, C. C., Ma, Y. F., Shannon, K. B., Chen, D. R., and Huang, Y. W. (2009). Toxicity of nano- and micro-sized ZnO particles in human lung epithelial cells. *J. Nanopart. Res.* **11,** 25–39.

Manzo, S., Rocco, A., Carotenuto, R., Picione Fde, L., Miglietta, M. L., Rametta, G., and Di Francia, G. (2010). Investigation of ZnO nanoparticles' ecotoxicological effects towards different soil organisms. *Environ. Sci. Pollut. Res. Int.* **18,** 756–763.

Mercer, R. R., Hubbs, A. F., Scabilloni, J. F., Wang, L. Y., Battelli, L. A., Schwegler-Berry, D., Castranova, V., and Porter, D. W. (2010). Distribution and persistence of pleural penetrations by multi-walled carbon nanotubes. *Part. Fibre Toxicol.* **7,** 28.

Miao, A. J., Zhang, X. Y., Luo, Z., Chen, C. S., Chin, W. C., Santschi, P. H., and Quigg, A. (2010). Zinc oxide-engineered nanoparticles: Dissolution and toxicity to marine phytoplankton. *Environ. Toxicol. Chem.* **29,** 2814–2822.

Oberdorster, G., Oberdorster, E., and Oberdörster, J. (2005). Nanotoxicology: An emerging discipline evolving from studies of ultrafine particles. *Environ. Health Persp.* **113,** 823–839.

Orr, G., Panther, D. J., Cassens, K. J., Phillips, J. L., Tarasevich, B. J., and Pounds, J. G. (2009). Syndecan-1 mediates the coupling of positively charged submicrometer amorphous silica particles with actin filaments across the alveolar epithelial cell membrane. *Toxicol. Appl. Pharmacol.* **236,** 210–220.

Orr, G., Panther, D. J., Phillips, J. L., Tarasevich, B. J., Dohnalkova, A., Hu, D. H., Teeguarden, J. G., and Poundsl, J. G. (2007). Submicrometer and nanoscale inorganic particles exploit the actin machinery to be propelled along microvilli-like structures into alveolar cells. *ACS Nano* **1,** 463–475.

Orr, G. A., Chrisler, W. B., Cassens, K. J., Tan, R., Tarasevich, B. J., Markillie, L. M., Zangar, R. C., and Thrall, B. D. (2011). Cellular recognition and trafficking of amorphous silica nanoparticles by macrophage scavenger receptor A. *Nanotoxicology* **5,** 296–311.

Porter, D., Sriram, K., Wolfarth, M., Jefferson, A., Schwegler-Berry, D., Andrew, M., and Castranova, V. (2008). A biocompatible medium for nanoparticle dispersion. *Nanotoxicology* **2,** 144–154.

Poynton, H. C., Lazorchak, J. M., Impellitteri, C. A., Smith, M. E., Rogers, K., Patra, M., Hammer, K. A., Allen, H. J., and Vulpe, C. D. (2011). Differential gene expression in Daphnia magna suggests distinct modes of action and bioavailability for ZnO nanoparticles and Zn ions. *Environ. Sci. Technol.* **45,** 762–768.

Sager, T. M., Porter, D. W., Robinson, V. A., Lindsley, W. G., Schwegler-Berry, D. E., and Castranova, V. (2007). Improved method to disperse nanoparticles for in vitro and in vivo investigation of toxicity. *Nanotoxicology* **1,** 118–129.

Sayes, C. M., Reed, K. L., and Warheit, D. B. (2007). Assessing toxicity of fine and nanoparticles: Comparing in vitro measurements to in vivo pulmonary toxicity profiles. *Toxicol. Sci.* **97,** 163–180.

Takenaka, S., Karg, E., Roth, C., Schulz, H., Ziesenis, A., Heinzmann, U., Schramel, P., and Heyder, J. (2001). Pulmonary and systemic distribution of inhaled ultrafine silver particles in rats. *Environ. Health Perspect.* **109**(Suppl. 4), 547–551.

Teeguarden, J. G., Hinderliter, P. M., Orr, G., Thrall, B. D., and Pounds, J. G. (2007). Particokinetics in vitro: Dosimetry considerations for in vitro nanoparticle toxicity assessments. *Toxicol. Sci.* **95,** 300–312.

Veranth, J. M., Kaser, E. G., Veranth, M. M., Koch, M., and Yost, G. S. (2007). Cytokine responses of human lung cells (BEAS-2B) treated with micron-sized and nanoparticles of metal oxides compared to soil dusts. *Part. Fibre Toxicol.* **4,** 2.

Wang, H., and Joseph, J. A. (1999). Quantifying cellular oxidative stress by dichlorofluorescein assay using microplate reader. *Free Radic. Bio. Med.* **27,** 612–616.

Wang, Z. L. (2004). Zinc oxide nanostructures: Growth, properties and applications. *J. Phys. Condes. Matter* **16,** R829–R858.

Warheit, D. B., Sayes, C. M., and Reed, K. L. (2009). Nanoscale and fine zinc oxide particles: Can in vitro assays accurately forecast lung hazards following inhalation exposures? *Environ. Sci. Technol.* **43,** 7939–7945.

Weaver, T. E., and Whitsett, J. A. (1991). Function and Regulation of expression of pulmonary surfactant-Associated proteins. *Biochem. J.* **273,** 249–264.

Wesselkamper, S. C., Chen, L. C., and Gordon, T. (2001). Development of pulmonary tolerance in mice exposed to zinc oxide fumes. *Toxicol. Sci.* **60,** 144–151.

Wick, P., Manser, P., Limbach, L. K., Dettlaff-Weglikowska, U., Krumeich, F., Roth, S., Stark, W. J., and Bruinink, A. (2007). The degree and kind of agglomeration affect carbon nanotube cytotoxicity. *Toxicol. Lett.* **168,** 121–131.

Wikenheiser, K. A., Vorbroker, D. K., Rice, W. R., Clark, J. C., Bachurski, C. J., Oie, H. K., and Whitsett, J. A. (1993). Production of immortalized distal respiratory epithelial-cell lines from surfactant protein-C simian virus-40 large tumor-antigen transgenic mice. *Proc. Natl. Acad. Sci. U.S.A.* **90,** 11029–11033.

Wong, S. W. Y., Leung, P. T. Y., Djurisic, A. B., and Leung, K. M. Y. (2010). Toxicities of nano zinc oxide to five marine organisms: Influences of aggregate size and ion solubility. *Anal. Bioanal. Chem.* **396,** 609–618.

Wu, W. D., Samet, J. M., Peden, D. B., and Bromberg, P. A. (2010). Phosphorylation of p65 is required for zinc oxide nanoparticle-induced interleukin 8 expression in human bronchial epithelial cells. *Environ. Health Persp.* **118,** 982–987.

Xia, T., Zhao, Y., Sager, T., George, S., Pokhrel, S., Li, N., Schoenfeld, D., Meng, H., Lin, S., Wang, X., *et al*. (2011). Decreased dissolution of ZnO by iron doping yields nanoparticles with reduced toxicity in the rodent lung and zebrafish embryos. *ACS Nano* **5,** 1223–1235.

Zhu, X., Wang, J., Zhang, X., Chang, Y., and Chen, Y. (2009). The impact of ZnO nanoparticle aggregates on the embryonic development of zebrafish (Danio rerio). *Nanotechnology* **20,** 195103.